Original article

Textile Research Journal

Textile Research Journal
0(00) 1–11

DOI: 10.1177/0040517517708536
journals.sagepub.com/home/trj

SAGE

Interlaminar reinforcement for enhancing low-velocity impact response of woven composites

AG Castellanos[1], Md S Islam[2], E Tarango[1], Y Lin[1] and P Prabhakar[3]

Abstract

This paper proposes a novel technique for improving the low-velocity impact response of woven composites, which involves synthesizing ZnO nanowires on dry woven carbon fabric layers. ZnO nanowire reinforcements were added to the interlaminar regions that are most susceptible to damage within layered composites, which were determined using finite element method analysis. Upon fabricating the laminates with and without ZnO nanowire interlaminar reinforcements, low-velocity impact responses were investigated next and the degree of damage was experimentally determined. The physical tests reveal that the samples with ZnO nanowires experience a lower degree of damage, up to a maximum of 25% for different impact energies, in comparison to the samples without ZnO nanowires. Therefore, the study presented in this paper shows the potential of using ZnO nanowires as interlaminar reinforcements for woven composites to improve their impact damage resistance.

Keywords

composites, surface modification, properties, nanowires, impact, delamination

Carbon fiber-reinforced woven composites consist of layers of woven carbon fabric reinforced in a polymer matrix material. The region between the layers of reinforcing fabric is a resin-rich region known as the ''interlaminar region,'' which is highly susceptible to damage and could lead to premature failure of the composite.[1] Specifically, loads like face impact or edgewise compression can cause significant damage in the interlaminar regions. Often, the residual strength of composites is drastically reduced by impact damage in the transverse direction due to the lack of reinforcement in the interlaminar regions. In this paper, a novel interlaminar reinforcing technique using ZnO nanowires is employed and their influence on the low-velocity impact response of woven carbon fiber-reinforced laminates is explored.

Low-velocity impacts can occur during manufacturing, tool dropping during maintenance activities, accidental impacts in-service, hail strikes, etc.[2–5] Such events can cause significant damage in the interior of these composites, with barely visible damage on the exterior. This is particularly dangerous, as barely visible damage (BVD) has the potential to cause catastrophic failure without warning. Dynamic impact is generally divided into low- or high-velocity impact.[6,7] Typical low-velocity impact occurs at a velocities below 10 m/s.[8] Common failure modes observed during low-velocity impact are fiber breakage, matrix cracking and delamination.[9–11] Of these, delamination is one of the most common failure mechanisms[12] observed during low-velocity impact,[13] which often results in the reduction of stiffness, strength, durability and stability of the composite, resulting in the global failure of the structure.[14,15]

[1]Department of Mechanical Engineering, University of Texas at El Paso, USA
[2]Department of Mechanical Engineering, Khulna University of Engineering and Technology, Bangladesh
[3]Department of Civil and Environmental Engineering, University of Wisconsin-Madison, USA

Corresponding author:
P Prabhakar, University of Wisconsin-Madison, 1415 Engineering Drive Madison, WI Wisconsin 53706, USA.
Email: pprabhakar4@wisc.edu

To increase the delamination resistance and extend the life of a composite structure, several through-thickness reinforcements have been investigated by earlier researchers. Sohn and Hu[16] explored chopped Kevlar® fibers as reinforcements in unidirectional composites. A 100% increase in the interlaminar fracture toughness value was observed, while the compressive strength appeared to reduce up to 15%. The compressive strength reduced from 652.2 MPa without reinforcement to 559.5 MPa with reinforcement. Ren et al.[17] investigated flocked C-fibers to increase the fracture toughness, which showed an improvement of around 900%. Despite the advantages, flock fibers can be shaken loose during handling, it is a time-consuming process and the quality of the reinforcement could be reduced as the fibers begin to lay flat on the surface of the fabric. Other methods, such as z-pinning and stitching, have shown to decrease the area of damage and increase the compression after impact (CAI) response. However, these methods appear to decrease the in-plane properties of the laminate due to undesired effects, such as fiber breakage and the creation of large resin pockets around a z-pin or thread.[18] Carbon nanotubes (CNTs) have also been proposed as potential through-thickness reinforcements. However, CNTs do not distribute uniformly throughout the fabric. Also, a decrease in the in-plane properties by nearly 55%[19] was reported due to damaged fibers, which is attributed to the high temperature (723°C) required for the reaction temperature of the dissolution of iron catalyst into the carbon fibers. Therefore, a low-temperature solution-based fabrication of zinc oxide (ZnO) nanowires as interlaminar reinforcement is explored in the current paper to avoid/reduce any such in-plane damage, while improving the through-thickness properties.

Previous researchers[20,21] have verified that ZnO nanowires have a strong chemical bonding to carbon fibers. ZnO nanowires have very strong interaction with carbon fibers, as previous studies have suggested.[22] Functional groups, such as hydroxyl, carbonyl and carboxylic acid, have been found in carbon fibers that create a strong chemical bonding with ZnO.[23–25] Composites with ZnO nanowires have 23 times higher impact energy absorption compared to pristine composites.[26] Also, ZnO nanowires have piezoelectric and semiconducting properties, which make them suitable for solar cells,[27] dynamic sensors[28] and energy-harvesting applications.[29] A recent study by Castellanos et al.[30] has shown that ZnO nanowires improve mode I (opening) interlaminar fracture toughness by approximately 74% and mode II (shear) interlaminar fracture toughness by approximately 28% for plain weave carbon composites.

Carbon fiber woven composites are studied in this paper. ZnO nanowires are synthesized on dry fabric and the composites are manufactured using the Vacuum Assisted Resin Transfer Molding (VARTM) process. The impact response and degree of damage of the laminates with and without ZnO nanowires are then compared to draw conclusions on the influence of interlaminar reinforcements. The paper is organized in the following sections: the second section, *Methods*, gives a description of the laminate manufacturing process, synthesis of ZnO nanowire on fabric, impact test and modeling is given. This is followed by the third section, the *Results and discussion*, where the modeling and experimental results are described and, finally, the fourth section 4 presents the conclusion.

Methods

Manufacturing

VARTM process for composite manufacturing. Woven composites with and without ZnO nanowires were manufactured by the VARTM process.[31] Laminates were fabricated by placing layers of dry carbon fabric in an aluminum mold with layers of flow media, breather and nylon peel ply, as shown in Figure 1(a). This was followed by enclosing the mold in a vacuum bag (see Figure 1(b)) and drawing it into vacuum in order to aid the infiltration of resin.

Laminates with 16 layers of dry fabric were manufactured according to the ASTM Standard D7136/D7136M.[32] Dry fabrics of woven plain weave (Figure 2(a)) were used as reinforcement with a mixture of vinyl ester resin and methyl ethyl ketone peroxide (MEKP) hardener as the matrix material. The resin was catalyzed with 1.25% MEKP (by weight) and mixed thoroughly for 1 minute, as recommended by the manufacturer. Samples with and without ZnO nanowires were manufactured together, as shown in Figure 2(b), to ensure that the curing conditions were identical. A total of five laminates of 12 in. (305 mm) by 12 in. (305 mm) were manufactured. From each laminate, six samples were obtained (three samples with ZnO nanowires and three without). A total of 30 samples were manufactured (15 samples with ZnO nanowires and 15 without ZnO nanowires). ZnO nanowires were synthesized on dry fabric at weak interlaminar regions suggested by the simulation of the impact test. From the simulation, the interlaminar regions with the highest stresses were deemed susceptible to delamination. More details about the simulation can be found in the *Impact modeling* section of this paper.

A cross-section of the manufactured laminate was examined under a scanning electron microscope (SEM) to obtain an average thickness of the effective

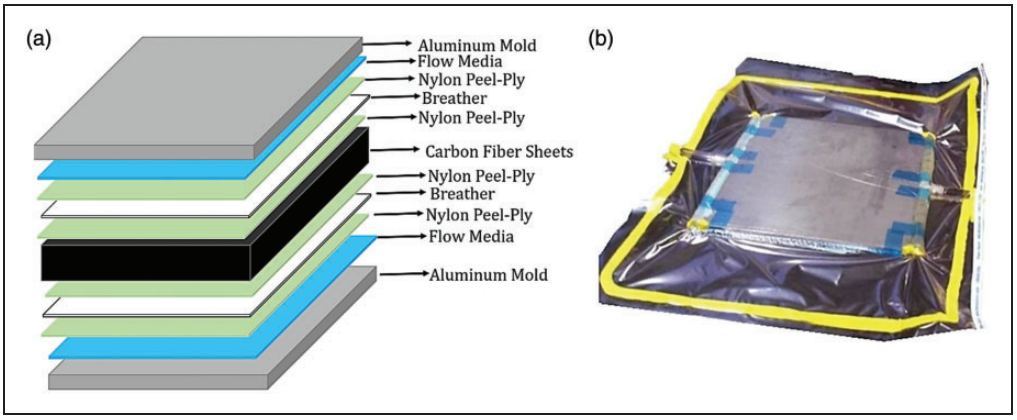

Figure 1. Vacuum Assisted Resin Transfer Molding configuration for the carbon woven composite.

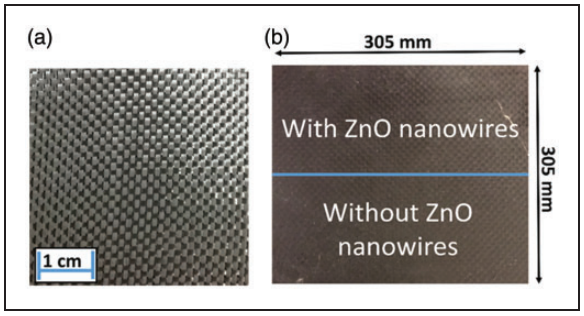

Figure 2. (a) Woven (plain weave) carbon fabric layer. (b) Schematic of a 12 in. by 12 in. manufactured laminate.

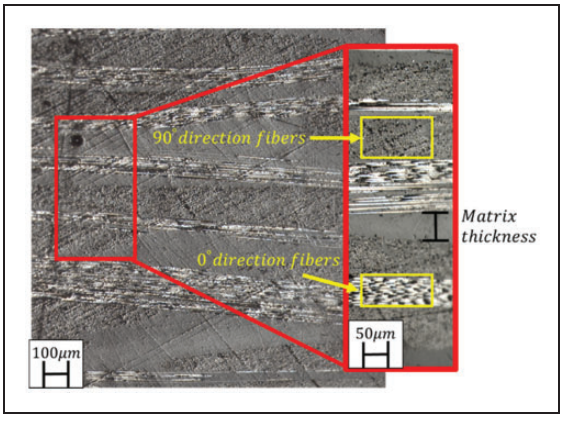

Figure 3. Cross-section of a laminated composite used to calculate the matrix thickness.

woven carbon fabric layers and interlaminar matrix regions, as shown in Figure 3. The average thickness of the matrix was 0.2 mm ± 0.01 mm. The synthesis of nanowires on dry fabric is described in the following section.

ZnO nanowire synthesis on dry fabric. ZnO nanowires added to the interlaminar regions more susceptible to damage were synthesized using a hydrothermal method. The synthesis was conducted in three steps: the seeding process, the growth process and post processing. For the seeding process, ZnO nanoparticles were formed by dissolving zinc acetate dehydrate (0.0125M) in ethanol at 50°C under vigorous stirring. Then, the solution was cooled down to room temperature and diluted with ethanol to a concentration of 0.0014M. A 0.02M NaOH ethanol solution was similarly prepared at 60°C and cooled to room temperature and diluted to a concentration of 0.0057M. The two solutions were then vigorously mixed at a growth temperature of 55°C at a volume ratio of 18:7.[33] ZnO nanoparticles were coated on a carbon fabric by means of dip coating in the mixture of the solutions.[21] After that, the carbon fabric was annealed at 150°C for 10 minutes to enhance the adhesion between the fibers and ZnO nanoparticles. For the growth process, an aqueous solution of zinc nitrate hydrate (0.025M) with hexamethylenetetramine (HMTA) (0.025M) was used as the solution for ZnO nanowire growth. The growth process was performed in a glass beaker with the solution temperature maintained at 90°C for 4 hours on a hot plate. For post processing, the carbon fabric was removed from the solution and rinsed with 18.2 MΩ water and then dried at 100°C.[21] Low-molecular-weight polyethylenimine (PEI, Aldrich, Mw = 25,000) was added to aid the uniform growth of nanowires.[34]

The morphology (diameter, length and orientation) and quality of ZnO nanowires synthesized on carbon fibers can be controlled through multiple parameters: temperature, solution concentration, ZnO nanoparticle size and growth time.[35] The temperature affects the growth time of the ZnO nanowires. That is, the growth of the ZnO nanowires will be slower if

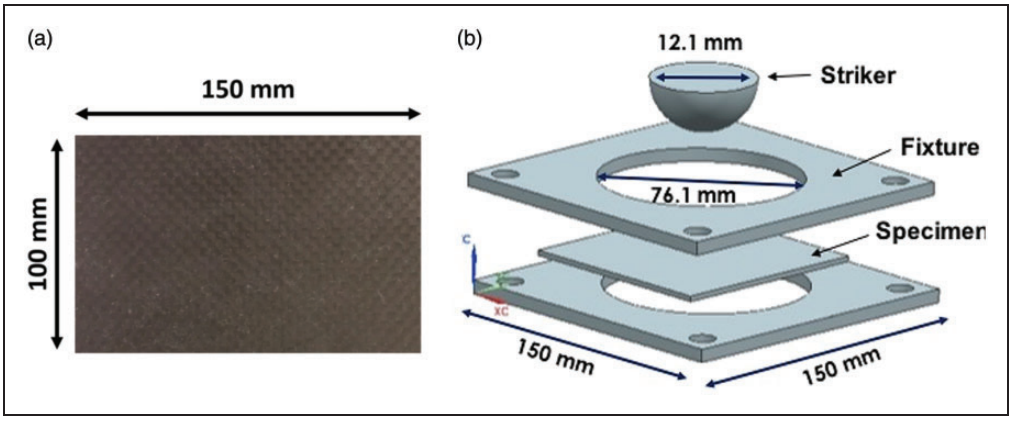

Figure 4. (a) Specimen dimensions (top view). (b) Schematic of the impact fixture.

the temperature is reduced. In addition, the solution concentration affects the length-to-diameter ratio and the growth rate. Further, the diameter and the length are directly proportional to the growth time. Also, a smaller size of nanoparticles yields smaller diameter nanowires. In the current study, the process parameters mentioned above resulted in an approximate final geometry of the ZnO nanowires of 50 nm diameter and 500 nm length.[21] The cost for manufacturing a 16-layer laminate of 12 in. long and 12 in. wide without nanowire reinforcement was approximately US$126.25. Adding nanowire reinforcements to the laminate increased the cost to US$137.47, which is approximately 9% as compared to the previous laminate.

Impact tests

Drop-weight impact tests were performed using a CEAST 9340 Drop Tower Impact System on rectangular laminate specimens of 6.0 in. (150 mm) length × 4.0 in. (100 mm) width (refer to Figure 4(a)) and thicknesses of 4.49 mm ± 0.08 mm. The laminates were clamped between two metal fixtures with a test area of 7.07 in^2 (45.6 cm^2). The impact load, using a hemispherical impactor (striker) with a mass of 3.01 kg and a diameter of 0.5 in. (12.7 mm), was concentrated at the center of the specimen in the out-of-plane direction[32] with kinetic energies of 2, 5, 10, 20 and 25 J for both types of samples (with and without ZnO nanowires). Kinetic energy is calculated based on the mass of the impactor and the impact velocity. Here, the mass of the striker was fixed to 3.01 kg. For a particular impact energy, the impact velocity and the striker falling height were adjusted accordingly by the Instron machine CEAST 9340. A schematic of an impact test is shown on Figure 4(b). Three samples were impacted for each impacted energy and sample type. Corresponding force–time, energy–time and force–displacement plots were obtained from each test.

Impact modeling

A 16-layer plain weave carbon laminate was modeled within the finite element method (FEM) framework using a commercially available software (ABAQUS) to determine the interlaminar regions that were most susceptible to impact damage. The laminate model consisted of 31 layers in total: 16 layers of effective plain woven carbon fabric reinforcement and 15 layers of matrix material, as shown in Figure 5.

Rectangular specimens of 6.0 in. (150 mm) long and 4.0 in. (100 mm) wide were used for experimental testing, which were clamped between circular ring metal fixtures, as shown in Figure 6. The outer diameter of the metal fixture was 4 in. (100 mm) and the inner diameter was 3 in. (76.2 mm). For the computational modeling, only the region of the laminate enclosed within the metal fixture was considered, as this was the main region influenced during low-velocity impact loading. A constant pressure of 0.2 MPa at the top and bottom of the laminate in the circular ring region was applied to simulate the clamping effect of the fixture.

Mechanical properties[36] of a plain weave carbon lamina used for initial simulations are shown in Table 1, where E_{ij} are the elastic moduli, ν_{ij} are the Poisson's ratios and G_{ij} are the shear moduli in different directions.

These mechanical properties were modified until the initial slope of the force–time graph of the simulation matched the slope of an experimental test impacted with the same energy as the computational model. Parametric studies revealed that the interlaminar regions prone to damage were always the same regions, regardless of the scaled lamina properties for this laminate. This is due to the same orthotropic properties and orientations of each lamina in the laminate. The mechanical properties used for the simulation are shown in Table 2.

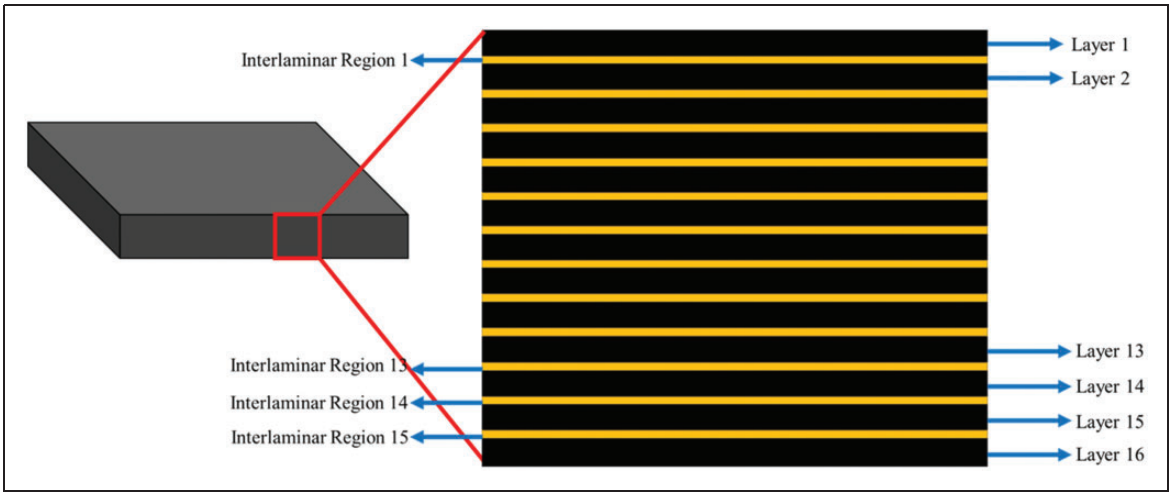

Figure 5. Schematic of the fabric layers and interlaminar regions of the laminate.

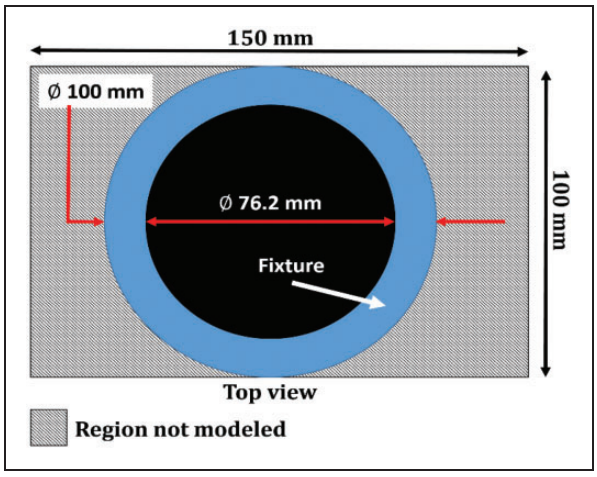

Figure 6. Top view of the specimen clamped by the impact metal fixture.

Table 1. Plain weave carbon lamina material constants used for the initial computational modeling

E_{11} (GPa)	E_{22} (GPa)	E_{33} (GPa)	ν_{12}	ν_{13}	ν_{23}	G_{12} (GPa)	G_{13} (GPa)	G_{23} (GPa)
48	48	1.94	0.3	0.3	0.3	0.94	0.765	0.765

Table 2. Plain weave carbon lamina material constants used for the computational modeling

E_{11} (GPa)	E_{22} (GPa)	E_{33} (GPa)	ν_{12}	ν_{13}	ν_{23}	G_{12} (GPa)	G_{13} (GPa)	G_{23} (GPa)
37.13	37.13	1.14	0.2	0.48	0.27	0.47	0.38	0.38

Individual layers of the laminate were modeled as homogenized material with orthotropic properties. Mechanical properties along the in-plane axes were considered equal and the out-of-plane properties (through-thickness direction) different, $E_{11} = E_{22} \neq E_{33}$, as shown in Table 2. The kinetic energy used for the simulation was 2 J. The impact velocity was calculated with the following equation

$$E_k = \frac{1}{2}mv^2 \quad (1)$$

where E_k is kinetic energy (J), m is striker mass (kg) and v is striker velocity (m/s)

A hemispherical striker was modeled as a half sphere following the requirements of the ASTM Standard D7136/D7136M to perform a drop-weight impact event. The striker was modeled as a rigid body and its motion was governed by a single reference point. A circular partition with an area of ≈ 7.0 in^2 (45.6 cm^2) (refer to Figure 7(a)) was created on the top and bottom faces of the laminate to simulate the circular aperture of the clamp. All the degrees of freedom of the nodes of the bottom and top clamp were restrained. Eight-noded three-dimensional (3D) elements (C3D8) were used to mesh the striker and the laminate. Finer mesh was used at the center of the circular region, as shown in Figure 7(b). Surface-to-surface contact between the striker and the impacted laminate surface was added using the contact algorithm in-built within the Explicit module of ABAQUS.

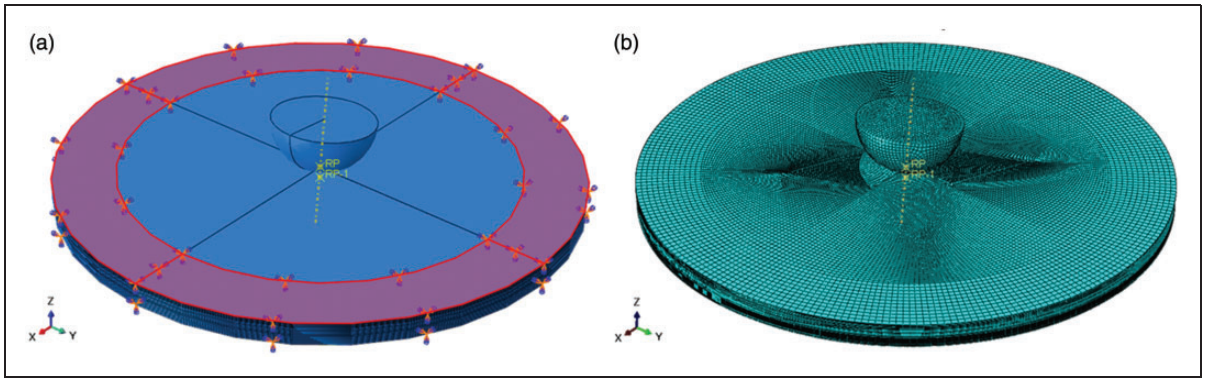

Figure 7. (a) Impact model of the specimen with boundary conditions. (b) Meshed model using C3D8 elements.

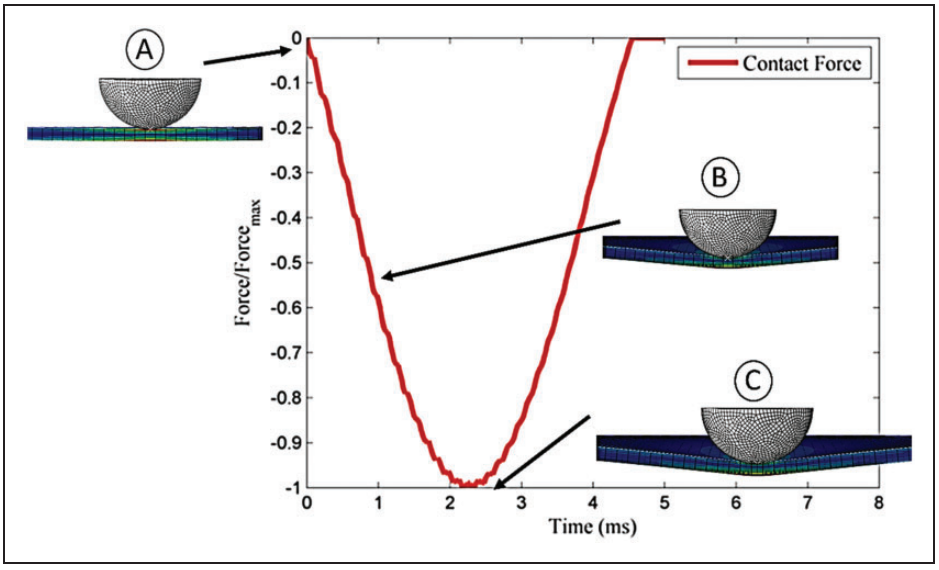

Figure 8. Normalized contact force versus time of the impact model.

Results and discussion

Computational modeling

The force–time response of the laminate subjected to 2 J impact energy was determined (refer to Figure 8). The time corresponding to the maximum contact force experienced by the impacted sample was determined using the normalized contact force–time plot shown in Figure 8, which was 2.3×10^{-3} s. The center element in the plane of each interlaminar region was chosen to plot the maximum principal stress–time response.

Figure 9(a) shows the maximum principal stresses corresponding to the peak impact force. The regions near the impacted face are under compression and the ones close to the back face are under tension. Figure 9(b) shows the normalized maximum principal stress–time plot of the interlaminar region that experienced higher stresses in comparison to other interlaminar regions. It was observed that Interlaminar Region 1 (underneath the impacted layer) and Interlaminar Regions 13–15 (three interlaminar regions towards the back surface of the laminate) experienced relatively higher stresses than the other interlaminar regions.

Interlaminar Region 1 experienced compressive stresses, which is represented by blue in Figure 9(a). Layers towards the back face of the laminate (close to Interlaminar Region 15) experienced tensile stresses, which is represented by red in Figure 9(a). Tensile stresses have been reported to cause more damage during an impact event.[37] Further, the material layer adjacent to the impacted surface experienced higher stresses due to the proximity of loading as well as the surface wave propagation known as the Rayleigh wave.[38] Hence, ZnO nanowire interlaminar reinforcements were

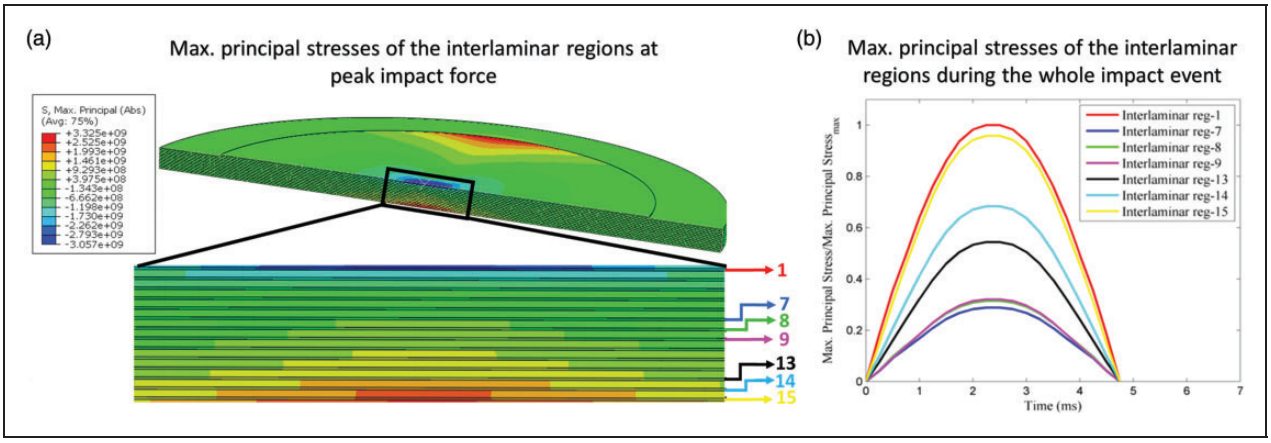

Figure 9. (a) Maximum principal stresses of the interlaminar regions at the peak impact force. (b) Normalized maximum principal stresses versus time of the interlaminar regions that exhibited higher stresses. (Color online only.)

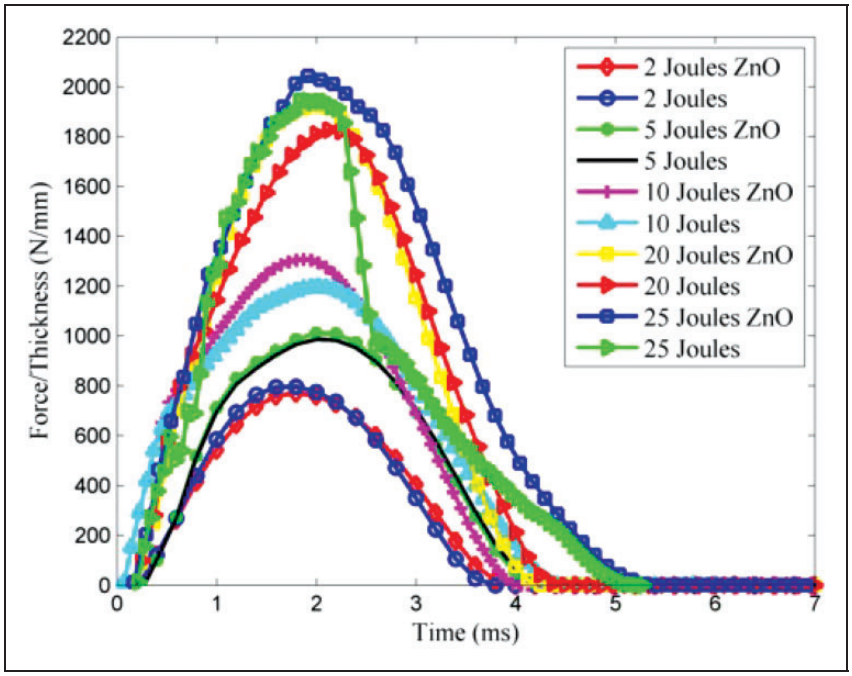

Figure 10. Normalized force–time response for one set of samples impacted at 2, 5, 10, 20 and 25 J energies.

added at the interlaminar regions that exhibited at least 50% of the maximum interlaminar stresses determined from the simulation.

Impact testing

The kinetic energies considered for the impact tests were 2, 5, 10, 20 and 25 J. Three samples were impacted with the same energy for nanowire-reinforced and unreinforced samples. Regions for nanowire interlaminar reinforcements were computationally determined from the *Computational modeling* section. For the experimental tests, the impact responses were evaluated in terms of visual damage of the impacted specimens and by calculating the degree of damage. The time, deformation, energy, force, velocity and voltage were recorded by the data acquisition system "CEAST DAS 8000 Junior" of the impact machine for each test conducted. Figure 10 shows the sample thickness normalized force–time responses from the impact tests of one set of samples with and without nanowire reinforcements impacted at different energies.

Table 3. Normalized peak force and maximum deflection for samples with and without ZnO nanowires

Energy (J)	Normalized peak force w/ZnO (N/mm)	Max. deflection w/ZnO (mm)	Normalized peak force w/o ZnO (N/mm)	Max. deflection w/o ZnO (mm)
2 J	641 ± 146	1.02 ± 0.04	629 ± 129	1.06 ± 0.04
5 J	813 ± 192	1.92 ± 0.33	812 ± 191	2.47 ± 0.67
10 J	1252 ± 51	3.06 ± 0.50	1122 ± 72	3.33 ± 0.40
20 J	1769 ± 141	4.17 ± 0.34	1684 ± 133	4.67 ± 0.54
25 J	1884 ± 241	4.73 ± 1.18	1844 ± 59	5.37 ± 1.23

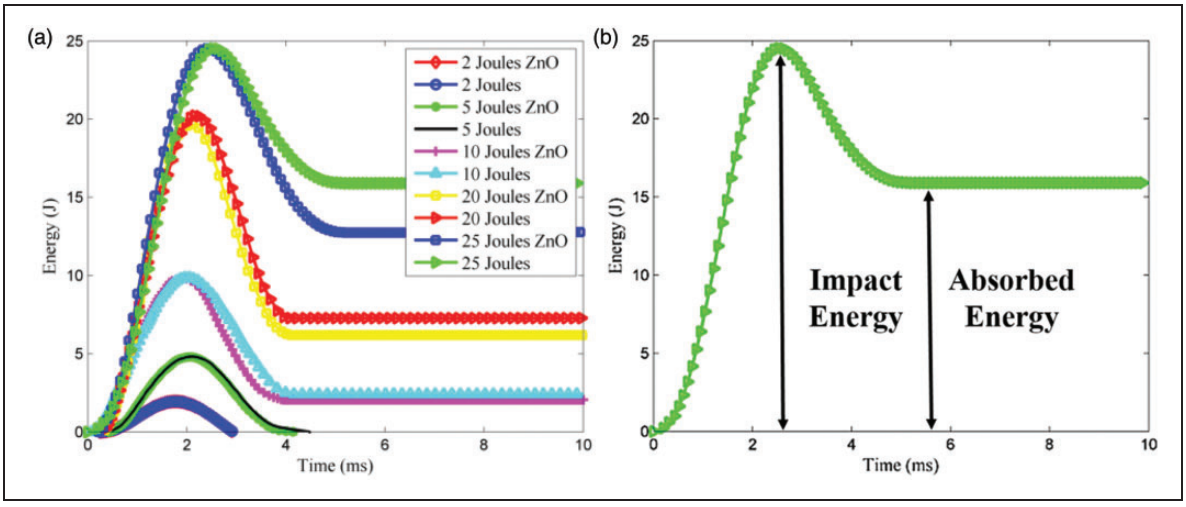

Figure 11. (a) Energy versus time graph. (b) Typical response of an energy versus time graph.

The force is generated by the contact of the striker with the impacted face of the sample, which is recorded with the data acquisition system of the impact machine. Table 3 shows the average peak force and average maximum deflection obtained for each impact energy. Predominantly, samples with ZnO nanowires displayed higher peak force and lower deflection than samples without ZnO. This implies that the load carrying capacity of the reinforced samples increased and the overall deformation of the laminate reduced as well.

Figure 11(a) shows representative energy–time responses of 10 specimens (five with and five without ZnO nanowire samples) that were impacted with the five energies mentioned in the previous section. A schematic of a typical energy–time response is shown in Figure 11(b), where the peak value corresponds to the impact energy and the plateau region represents the absorbed energy.

In Figure 11(a), the difference between the absorbed energy (plateau region) and the impacted energy appears to increase with increasing impact energies. In addition, the samples without nanowires manifested higher absorbed energy for a particular impact energy, as seen in Figure 11(a). For this reason, the specimens without nanowires experienced more damage.

Further, to measure the damage experienced by the impacted specimens, the degree of damage[39] was calculated using the equation

$$D = \frac{Absorbed\ Energy}{Impact\ Energy} \tag{2}$$

Table 4 shows the average calculated degree of damage for each impact energy for samples with and without nanowire reinforcement. For impact energies 5, 10, 20 and 25 J, the samples with nanowires manifested lower values of D than the samples without ZnO nanowires, with up to 25% reduction. It should be noted that the degree of damage was zero for specimens impacted with 2 J energy, which indicates that no damage was imparted to those laminates and the striker rebounded from the impacted surface. Hence, ZnO nanowire reinforcement showed an improvement in damage resistance for low-velocity impact loading.

Images of the impacted laminates were obtained for the samples with and without ZnO nanowires to visually evaluate the pattern and extent of damage. Laminate cross-sections at the site of impact were examined using a SEM with 15 kV potential. An average of 70 magnified images at a scale of 500 µm per cross-section were stitched together to generate a larger image of the cross-section. Failure mechanisms of the laminate under impact are enclosed within red rectangular boxes in Figure 12, where delamination was identified as the main damage mode.

Laminates impacted at 2 J energy were not investigated for internal damage occurrence, as the striker rebounded from the impacted surface with zero degree of damage. For 5, 10 and 20 J, the majority of the damage imparted was internal to the laminate and barely visible on the surfaces. Thus, impacted samples were cut along their cross-section at the site of impact for further internal analysis. Cross-sectional images of the samples impacted at 5 J energy are shown in Figures 12(a) and (b) for specimens with and without nanowires, respectively. The sample without nanowires exhibited delamination and matrix cracks at the first interlaminar region, whereas the specimen with nanowires did not exhibit delamination. This suggests a strong bond between the layers of fabric due to ZnO nanowire reinforcement at that site.

Images of the cross-section of samples impacted at 10 J energy are shown in Figures 12(c) and (d) for samples with and without nanowires, respectively. The specimen with nanowires exhibited a delamination at the third interlaminar region, that is, between the third and fourth layers of fabric. The specimen without ZnO nanowires exhibited delamination at the first interface of the laminate along with fiber fracture in the first layer and at the back face of the composite. Cross-sectional images of the samples impacted at 20 J energy are shown in Figures 12(e) and (f) for the specimens with and without nanowires, respectively. The specimen with ZnO nanowires exhibited delamination at the second (between the second and third layers of fabric) and 13th (between the 12th and 13th layers of dry fabric)

Table 4. Percentage change in the degree of damage values for samples with and without ZnO nanowires

Energy (J)	*D*, sample w/ZnO	*D*, sample w/o ZnO	Percentage change
5 J	0.29 ± 0.03	0.21 ± 0.04	$23\% \pm 0.02$
10 J	0.44 ± 0.03	0.35 ± 0.02	$22\% \pm 0.03$
20 J	0.58 ± 0.01	0.44 ± 0.03	$25\% \pm 0.02$
25 J	0.71 ± 0.04	0.53 ± 0.06	$24\% \pm 0.02$

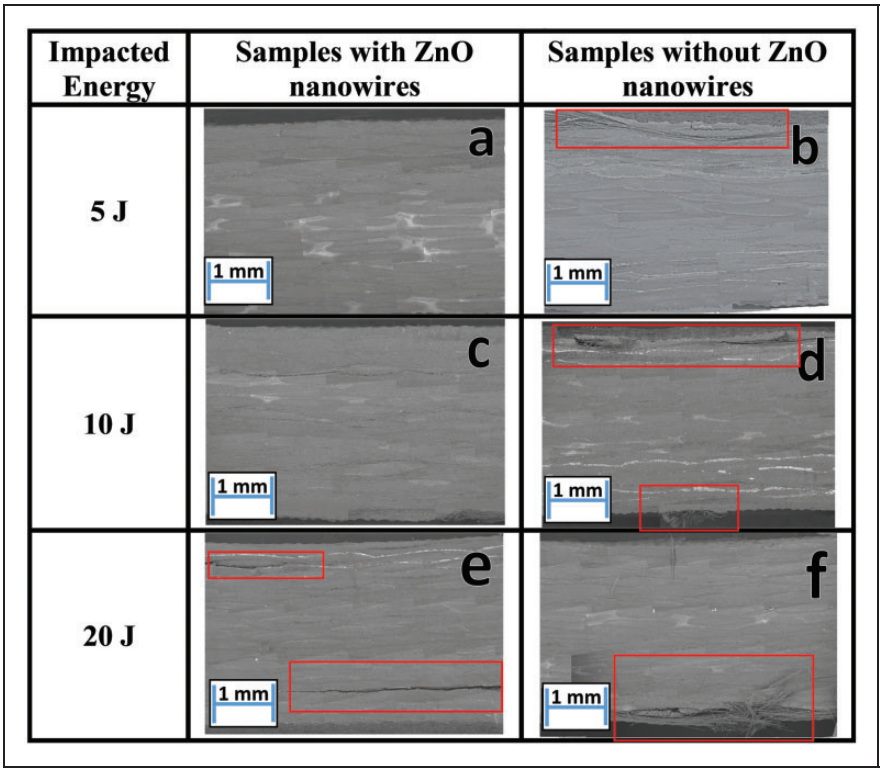

Figure 12. Cross-section of the specimens impacted at 5, 10 and 20 J for samples with and without ZnO nanowires.

interlaminar regions. The sample without ZnO nanowires exhibited multiple delaminations and fiber breakage towards the non-impacted surface of the laminate. The overall delamination appears to have reduced along with shifting of the interlaminar damage regions due to the nanowire reinforcements. A future work would involve reinforcing every interlaminar region to capture the overall influence.

A combination of fiber breakage, matrix cracking and delamination damage modes was observed for the samples impacted at 25 J energy. The top impacted surface of the laminate without nanowires exhibited a larger damage area as compared to the sample with nanowires. At the non-impacted surface, the sample without nanowires exhibited a long radial crack with fiber breakage, while the sample with nanowire only exhibited matrix cracks and minimal fiber breakage. However, for these samples, the interplay between different failure mechanisms is difficult to evaluate based on the images of the post failed samples.

Conclusion

A novel fabrication technique for imparting ZnO nanowire interlaminar reinforcements in woven carbon fiber-reinforced polymer composites was presented in this paper. The objective was to improve the out-of-plane impact response of the laminates without degrading the in-plane properties. A computational model was developed within the FEM framework to identify the interlaminar regions that are most susceptible to damage. Interlaminar reinforcements were then synthesized along the chosen interfaces, followed by laminate fabrication using the VARTM process. Low-velocity impact responses of carbon woven composites with and without ZnO nanowire interlaminar reinforcements were investigated next and the degree of damage was experimentally determined. Key findings of the research presented in this paper are as follows:

1. the impact tests revealed that the samples with ZnO nanowires experienced a lower degree of damage, up to a maximum of 25% for different impact energies, in comparison to the samples without ZnO nanowires for a range of impact energies between 5 and 25 J;
2. an increase in the impact peak load and reduction in maximum deflection was observed from the impact tests between samples with and without nanowire reinforcement;
3. a low absorption of energy by the samples with ZnO nanowires was observed, which can be attributed to the bridging and resistance of failure initiation caused by the ZnO nanowires at the interlaminar regions;
4. a shift in delamination regions were also observed in few cases, which corroborates the positive influence of nanowire reinforcement on resisting delamination.

Even though the improvement in the impact response is not drastic (approximately 25%), it can be improved further by exploring the wide range of nanowire synthesis parameters, such as temperature, solution concentration, ZnO nanoparticle size and growth time, as well as reinforcing all interlaminar regions. The current study serves as a preliminary work for further investigation into ZnO nanowires as potential interlaminar reinforcements for woven composites for improving their impact damage resistance. These nanowires have shown great potential for preventing or minimizing the degree of damage, which would improve the damage tolerance of composite structures.

Acknowledgement

The authors would like to acknowledge the support through the DoD HBCU/MI Basic Research Grant (W911NF-15-1-0430) to conduct the research presented in this paper.

Declaration of conflicting interests

The authors declared no potential conflicts of interest with respect to the research, authorship and/or publication of this article.

Funding

The authors disclosed receipt of the following financial support for the research, authorship, and/or publication of this article: This work was supported by a DoD HBCU/MI Basic Research Grant (W911NF-15-1-0430).

References

1. Wicks S, Wang W, Williams MR, et al. Multi-scale interlaminar fracture mechanisms in woven composite laminates reinforced with aligned carbon nanotubes. *Compos Sci Technol* 2014; 100: 128–135.
2. Julias A and Murali V. Effect of carbon fiber position on the impact behavior of glass/carbon fiber hybrid composite laminates. *Int J Appl Eng Res* 2014; 9: 9103–9106.
3. Safri S, Sultan M, Yidris N, et al. Low velocity and high velocity impact test on composite materials – a review. *Int J Eng Sci* 2014; 3: 50–60.
4. Malhotra A and Guild FJ. Impact damage to composite laminates: effect of impact location. *Appl Compos Mater* 2014; 21: 165–177.
5. Kostopoulos V, Baltopoulos A, Karapappas P, et al. Impact and after-impact properties of carbon fibre reinforced composites enhanced with multi-wall carbon nanotubes. *Compos Sci Technol* 2010; 70: 553–563.
6. Sjoblom P. Simple design approach against low velocity impact damage. In: *Proceedings of the 32nd SAMPE*

symposium, Anaheim, CA, Ralph Carson, 6–9 April 1987, pp.529–539. Covina, Calif.: The Society.
7. Shivakumar K, Elber W and Illg W. Prediction of impact force and duration due to low velocity impact on circular composite laminates. *J Appl Mech* 1985; 52: 674–680.
8. Cantwell W and Morton J. Impact perforation of carbon-fiber reinforced plastics. *Compos Sci Technol* 1990; 38: 119–141.
9. Abrate S. Impact on laminated composites: recent advances. *Appl Mech Rev* 1994; 47: 517–544.
10. Caprino V, Lopresto V, Scarponi C, et al. Effect of ZnO nanowire morphology on the interfacial strength of nanowire coated carbon fibers. *Compos Sci Technol* 1999; 59: 2279–2286.
11. Karakas R, Erbil E and Mehmet A. Impact characterization of glass/epoxy composite plates: an experimental and numerical study. *Composites Part B* 2010; 41: 388–395.
12. Serenest A. Overview on the experimental investigations of the fracture tough-ness in composite materials. *J Eng Mater Technol* 2011; 100: 1–19.
13. Kim J-K and Sham M-L. Impact and delamination failure of woven-fabric composites. *Compos Sci Technol* 2000; 60: 745–761.
14. Sheer T-W and Pan Y-H. Impact resistance and damage characteristic of composite laminates. *Compos Struct* 2003; 62: 193–203.
15. Babe S and Shiva HK. Impact analysis of laminated composite on glass fiber and carbon fiber. *Int J Emerg Technol Adv Eng* 2014; 4: 824–829.
16. Sohn M and Hu X. Processing of carbon fibre/epoxy composites with cost-effective interlaminar reinforcement. *Compos Sci Technol* 1998; 58: 211–220.
17. Ren J, Kim YK and Rice J. Comparing the fracture toughness of 3-D braided preform composites with z-fiber reinforced laminar composites. *Text Res J* 2011; 81: 335–343.
18. Sager RJ, Klein PJ, Davis DC, et al. Interlaminar fracture toughness of woven fabric composite laminates with carbon nanotube/epoxy interleaf films. Epub ahead of print 21 March 2011. DOI: 10.1002/app.33479.
19. Qian H, Bismarck A, Greenhalgh E, et al. Hierarchical composites reinforced with carbon nanotube grafted fibers: the potential assessed at the single fiber level. *Chem Mater* 2008; 95: 1862–1869.
20. Kong K, Deka BK, Kwak SK, et al. Processing and mechanical characterization of ZnO polyester woven carbon- fiber composites with different ZnO concentrations. *Composites Part A* 2013; 555: 152–160.
21. Lin Y, Ehlert G and Sodano H. Increased interface strength in carbon fiber composites through ZnO nanowire interphase. *Adv Funct Mate* 2009; 19: 2654–2660.
22. Crook S, Dhariwal H and Thornton G. HREELS study of the interaction of formic acid with ZnO(1010) and ZnO(0001)-O. *Surf Sci* 1997; 382: 19–25.
23. Dilsiz N and Wightman JP. Surface analysis of unsized and sized carbon fibers. *Carbon* 1999; 37: 1105–1114.
24. Dilsiz N and Wightman JP. Effect of acid-base properties of unsized and sized carbon fibers on fiber/epoxy matrix adhesion. *Colloids Surf A Physicochem Eng Asp* 2000; 164: 325–336.
25. Turgeman R, Gershevitz O, Deutsch M, et al. Crystallization of highly oriented ZnO microrods on carboxylic acid-terminated SAMs. *Chem Mater* 2005; 17: 5048–5056.
26. Hwang H, Malakooti M, Patterson B, et al. Increased interyarn friction through ZnO nanowire arrays grown on aramid fabric. *Compos Sci Technol* 2014; 107: 75–81.
27. Baxter JB and Eray SA. Nanowire-based dye-sensitized solar cells. *Appl Phys Lett* 2005; 86: 053114 1–3.
28. Wang SD, Song JH, Liu J, et al. Direct-current nanogenerator driven by ultrasonic waves. *Science* 2007; 316: 102–105.
29. Wang ZL and Song J. Piezoelectric nanogenerators based on zinc oxide nanowire arrays. *Science* 2006; 312: 242–246.
30. Castellanos A, Islam MS, Shuvo M, et al. Nanowire reinforcement of woven composites for enhancing interlaminar fracture toughness. *J Sandwich Struct Mater*. Epub ahead of print 22 July 2016. DOI: 10.1177/1099636216650989.
31. Chittajallu K. *Computational modeling of the vacuum assisted resin transfer molding (VARTM) process*. Thesis, Clemson University.
32. ASTM D7136/D7136M-15:2015. Standard test method for measuring the damage resistance of a fiber-reinforced polymer matrix composite to a drop-weight impact event.
33. Ehlert GJ and Sodano H. *Development of a zinc oxide nanowire interphase for enhanced structural composites*. Doctoral Dissertation. Retrieved from: US National Library of Medicine National Institutes of Health, 2009, pp.1–247.
34. Hu Z, Oskam G and Searson P. Influence of solvent on the growth of ZnO nanoparticles. *J Colloid Interface Sci* 2003; 263: 545–460.
35. Galan U, Lin Y, Ehlert G, et al. Effect of ZnO nanowire morphology on the interfacial strength of nanowire coated carbon fibers. *Compos Sci Technol* 2011; 71: 946–954.
36. Justusson BP. *The response of textile composites subjected to elevated loading rates*. PhD Thesis, University of Michigan, 2015.
37. Ullah H and Silberschmidt VV. Dynamic large-deflection bending of laminates. *Dyn Deform Damage Fract Compos Mater Struct* 2016; 1: 559–582.
38. McLaskey GC and Glaser SD. High-fidelity conical piezoelectric transducers and finite element models utilized to quantify elastic waves generated from ball collision. *Sensors and Smart Structures Technologies for Civil, Mechanical, and Aerospace Systems* 2009; 7292: 9–16.
39. Belingardi G, Cavatorta MP and Paolino DS. Repeated impact response of hand lay-up and vacuum infusion thick glass reinforced laminates. *Int J of Imp Eng* 2008; 35: 609–619.